Received 23 October 2023; revised 2 December 2023; accepted 20 December 2023. Date of publication 25 December 2023; date of current version 29 January 2024. The review of this article was arranged by Editor P. Pavan.

Digital Object Identifier 10.1109/JEDS.2023.3347049

2.1 W/mm Output Power Density at 10 GHz for H-Terminated Diamond MOSFETs With (111)-Oriented Surface

BING QIAO[1,2,3], PENGFEI DAI[1,2], XINXIN YU[1,2], ZHONGHUI LI[1,2,3], RAN TAO[1,2], JIANJUN ZHOU[1,3], RUI SHEN[1,2,3], AND TANGSHENG CHEN[1,3]

1 Nanjing Electronic Devices Institute, Nanjing 210016, China
2 CETC Key Laboratory of Carbon-Based Electronics, Nanjing 210016, China
3 National Key Laboratory of Solid-State Microwave Devices and Circuits, Nanjing 210016, China

CORRESPONDING AUTHORS: X. YU AND Z. LI (e-mail: yuxx711@126.com; zhonghuili@126.com)

ABSTRACT This paper presents high performance hydrogen-terminated diamond MOSFETs fabricated on a (111)-oriented single-crystal diamond substrate. The diamond surface was passivated by a high-quality Al_2O_3 grown by ALD at 350°C as well as a secondary passivation layer Si_3N_4 deposited by PECVD. After passivation, a low ohmic contact resistance R_c of 0.5 Ω·mm was obtained and the 2DHG sheet density was as high as 1.0×10^{13} cm^{-2} with a corresponding mobility of 104 cm^2 /V·s. The fabricated diamond MOSFET with gate length of 0.5 μm showcased a high current density of 750 mA/mm, a low on-resistance of 24 Ω·mm, and a high off-state breakdown voltage of 117 V. Thanks to the high current density and low on-resistance, a record high output power density of 2.1 W/mm was achieved at 10 GHz with drain biased at a low voltage of −30 V. These results demonstrate that the output current and output power can be improved by using a (111)-oriented diamond, which is benefit for high-frequency and high-power RF devices.

INDEX TERMS Hydrogen-terminated, (111)-oriented diamond, output power.

I. INTRODUCTION

As the representative of ultra-wide bandgap semiconductors, diamond is known as the ultimate semiconductor for its exceptional characteristics such as high breakdown electric field (10 MV/cm), high thermal conductivity (22 W/cm·K), and high carrier mobility (4500 cm^2/V·s for electrons and 3800 cm^2/V·s for holes) [1], [2], [3], making it a superior candidate for high-frequency and high-power devices. However, almost all purities such as boron and phosphorus in diamond have very high activation energies and they are difficult to be ionized at room temperature [4]. Thus, it is hard to achieve high performance RF devices by using the conventional bulk doping process [5], [6]. It was not until 1994 that the first hydrogen terminated diamond (H-diamond) metal semiconductor field-effect transistor (MESFET) by utilizing a two-dimensional-hole-gas (2DHG) channel was reported [7], which makes the H-diamond RF devices develop rapidly in the next three decades for its high performance 2DHG channels. To date, the diamond MOSFETs with record cutoff frequency (f_T) of 70 GHz, maximum oscillation frequency ($f_{\max}$) of 120 GHz, output power density of 4.2 W/mm at 2 GHz have been achieved by using the hydrogen termination technique [8], [9], [10].

The 2DHG density of the H-diamond is not only related to the hydrogenation process, but also depends on the orientation of the diamond surface. A higher density 2DHG can be achieved on a (111)-oriented diamond for its high C-H dipole charge density, which is beneficial for decreasing the on-resistance and improving the current density of the H-diamond MOSFETs [11], [12]. It implies that the power output characteristics can be improved by using a (111)-oriented H-diamond for its high current density. However, (111)-oriented diamonds are hard to be acquired and most of the reported H-diamond devices were fabricated on (001)- or (110)-oriented substrates. Only a few H-diamond MOSFETs on (111)-oriented surfaces were reported, and a high current density of over 1 A/mm and

© 2024 The Authors. This work is licensed under a Creative Commons Attribution-NonCommercial-NoDerivatives 4.0 License.
For more information, see https://creativecommons.org/licenses/by-nc-nd/4.0/

a high output power density of 3.6 W/mm at 1 GHz were achieved [13].

In our previous work, we have reported a H-diamond MOSFET on (001)-oriented surface and an output power density of 1.26 W/mm was achieved at frequency of 10 GHz [14]. In this work, a (111)-oriented H-diamond substrate was utilized to fabricate the diamond MOSFETs to reduce the on-resistance and improve the output current density. The Al_2O_3/Si_3N_4 bilayer passivation were employed to passivate the 2DHG channels, which is similar to that in our previous work [14], [15]. Attributing to the high performance 2DHG channels on the (111)-oriented diamond, the passivated channel sheet resistance was significantly reduced and the current density was improved from 561 mA/mm to 750 mA/mm, which contributes the great improvement in the output power density from 1.26 W/mm to 2.1 W/mm at the same operating voltage of −30 V.

II. DEVICE FABRICATION

The diamond MOSFETs were fabricated on a (111)-oriented single-crystal diamond substrate with a size of about $5\times5\times0.4$ mm^3. The surface root mean square (RMS) roughness was measured to be about 1 nm for the measurement area of 5 μm×5 μm by an atomic force microscopy (AFM). The diamond surface was exposed to hydrogen plasma in a microwave plasma chemical vapor deposition (MPCVD) system at 700 °C with power of 2.2 kW for 10 minutes to produce high density C–H bonds. Subsequently, the diamond was cooled down to room temperature in H_2 atmosphere.

After the diamond was exposed to air for more than 24 h, a 50 nm thick Au film was deposited on the hydrogen-terminated surface by the electron beam evaporation (EBE). The source, drain and channel regions were protected by the photoresist and the unmasked regions were removed by using the KI/I_2 solution. The oxygen plasma treatment with power of 300 W was carried out for 5 minutes to achieve device isolations with surface C-H bonds converted to C-O bonds. Afterwards, the source-to-drain spacings were defined by the electron beam lithography (EBL), and the Au film was removed by wet etching in diluted KI/I_2 solution. After the electron beam resist was removed, a 50 nm thick Al_2O_3 was deposited as the gate dielectric by atomic layer deposition (ALD) at 350°C with the trimethylaluminum and water used as the reactants. Before Al_2O_3 deposition, the diamond was annealed at 350°C in situ for 15 minutes to remove the surface absorbates. Afterwards, a 100 nm thick Si_3N_4 was deposited as a second passivation layer via plasma enhanced chemical vapor deposition (PECVD) at 250°C. The T-shaped gates were fabricated by a two-step EB lithography and selectively etching. The first EB lithography was used to define the gate foot and the unmasked Si_3N_4 was etched away by inductively coupled plasma (ICP). The second EB lithography was utilized to define the gate-head and a 20/500 nm Ti/Au metal stack was deposited as the gate metals. The detailed process was reported in our previous works [14], [16]. Finally, the Al_2O_3/Si_3N_4 contact windows were etched away by ICP and another 20/500 nm Ti/Au metal stack was evaporated to connect the pads with the source, drain and gate electrodes, respectively.

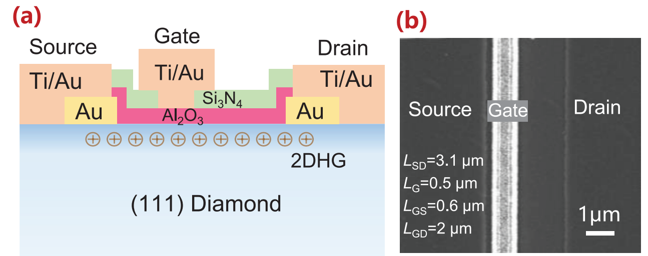

FIGURE 1. (a) The cross-sectional schematic structure and (b) enlarged SEM photo of the H-diamond MOSFET on (111)-oriented surface.

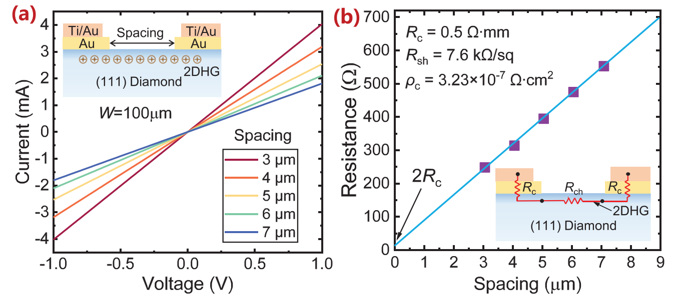

FIGURE 2. (a) The I-V curves of the ohmic electrode pairs with different spacings, (b) the resistances of the two adjacent ohmic electrodes versus their spacings.

Fig. 1(a) shows the cross-sectional schematic structure of the fabricated H-diamond MOSFET. The gate length L_G, gate-source spacing L_{GS}, and gate-drain spacing L_{GD} were about 0.5 μm, 0.6 μm and 2 μm, respectively, as shown in the SEM image in Fig. 1(b).

III. RESULTS AND DISCUSSION

The direct current characteristics of the H-diamond MOSFETs were measured via an Agilent B1500A semiconductor parameter analyzer. The ohmic contact characteristics were characterized by the transmission line method (TLM). The ohmic electrode spacings were varied from 3 μm to 7 μm with a step of 1 μm, and their widths were fixed at 100 μm. Fig 2(a) shows the I-V curves of the electrode pairs with different spacings. The resistances of the two adjacent ohmic electrodes extracted from Fig. 2(a) were well in linear relationship with their spacings, as shown in Fig. 2(b). The ohmic contact resistance R_c was calculated as low as 0.5 Ω·mm and the sheet resistance of the channel R_{sh} was 7.6 kΩ/sq, resulting in a low specific contact resistance ρ_c of 3.23×10^{-7} $\Omega\cdot cm^2$. Comparing with that of 5.81×10^{-6} $\Omega\cdot cm^2$ in our previous work, the ρ_c was dramatically reduced by an order of magnitude [12]. It is demonstrated that a favorable ohmic contact has been achieved on the (111)-oriented H-diamond surface.

To characterize the carrier transport performance of the Al_2O_3 passivated (111)-oriented H-diamond, the long-channel devices with gate length of 50 μm were fabricated

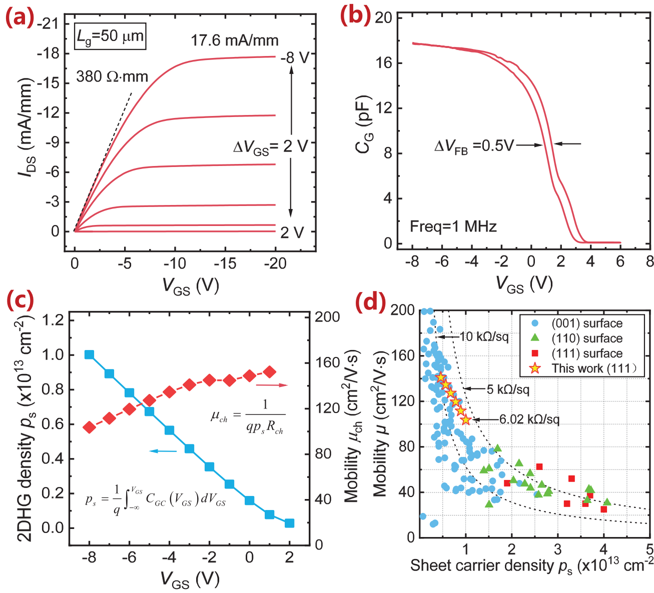

FIGURE 3. (a) The direct output current and (b) the C-V characteristics of the H-diamond MOSFET with gate length of 50 μm. (c) The 2DHG density and mobility versus the gate voltage. (d) The 2DHG density and mobility on H-diamonds with different orientations.

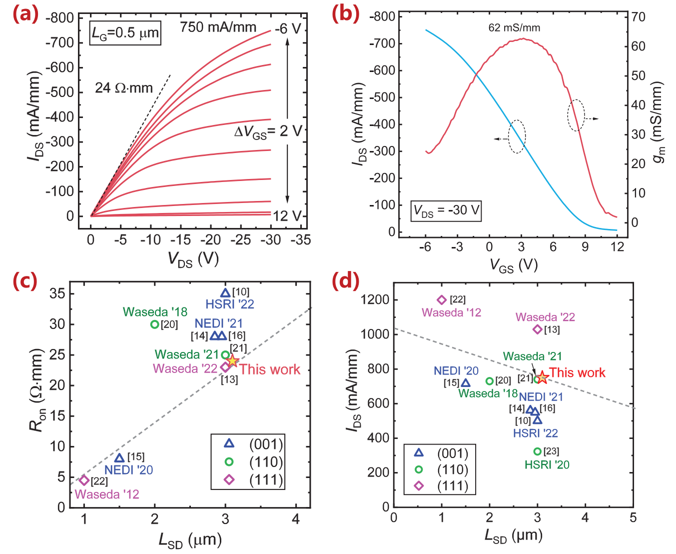

FIGURE 4. (a) The direct current output characteristics and (b) the transfer characteristics of the H-diamond MOSFET with gate length of 0.5 μm. (c) The on-resistance and (d) current density of the H-diamond MOSFETs with different surface orientations.

on the same substrate. The L_{GS} and L_{GD} were both 5 μm, and the gate width was 200 μm. Fig. 3(a) shows the direct current (DC) output curves of the long channel device and the current density was 17.6 mA/mm at $V_{GS} = -8$ V and V_{DS}=−20 V. The on-resistance was extracted as 380 Ω·mm. As the R_c and R_{sh} of the ungated channel were 0.5 Ω·mm and 7.6 kΩ/sq, the channel sheet resistance R_{ch} under the gate was calculated to be about 6.06 kΩ/sq. It indicates that the 2DHG concentration was enhanced at $V_{GS} = -8$ V and its sheet resistance was lower than that outside the gate. The C-V curves were measured by sweeping the gate voltage from −8 V to 6 V in double directions at a frequency of 1 MHz, as the results shown in Fig. 3(b). It was observed that there was a hysteresis and the flat band difference was about 0.5 V [17], which may be attributed to the interface states at the H-diamond/Al_2O_3 interface. By integrating the C-V curve, the hole density at each gate voltage can be obtained [18], [19]. Based on the extracted R_{ch} of the channel under the gate and the 2DHG density p_s, the 2DHG mobility μ_{ch} under the channel can be calculated, as the formulas and results shown in Fig. 3(c). At V_{GS} of −8 V, the maximum 2DHG sheet density was as high as 1.0×10^{13} cm^{-2} with a corresponding mobility of 104 cm^2/V·s. With the 2DHG density decreased to 4.6×10^{12} cm^{-2} at V_{GS} of −3 V, the mobility was significantly improved to 141 cm^2/V·s. It indicates that high performance 2DHG channels with high hole concentration and high mobility can be achieved on (111)-oriented diamonds. Fig. 3(d) demonstrates the 2DHG mobilities versus their sheet densities for the H-diamonds with various orientations [11], [12]. It is observed that the 2DHG density for the Al_2O_3 passivated (111)-oriented H-diamond is much lower than the previous reported values for (111)- or (110)-oriented H-diamonds, which may be attributed to the decrease of 2DHG density after Al_2O_3 passivation. However, the 2DHG mobility was significantly improved and a low 2DHG sheet resistance of 6.02 kΩ/sq was realized, which is lower than that on most (001)-oriented H-diamonds. It implies that a low sheet resistance 2DHG channel can be obtained on (111)-oriented H-diamond even with Al_2O_3 passivation.

Fig. 4(a) shows the DC output characteristics of the double-finger H-diamond RF MOSFET with gate length of 0.5 μm and total gate width of 100 μm. The device exhibits a high output current density of 750 mA/mm and a low on-resistance R_{on} of 24 Ω·mm at V_{GS}=−6 V. The transfer characteristics of the H-diamond MOSFET were measured at V_{DS} of −30 V, as the results shown in Fig. 4(b). The threshold voltage was about 12 V and the peak transconductance was 62 mS/mm, which is much larger than those with thicker Al_2O_3 gate dielectrics [20], [21]. Comparing with those on (001)- or (110)-oriented H-diamonds, the MOSFETs with (111)-oriented surfaces always demonstrated reduced R_{on} and improved current densities, as shown in Figs. 4(c) and (d) [10], [13], [14], [15], [16], [17], [18], [19], [20], [21], [22], [23]. It indicates that the 2DHG on (111)-oriented H-diamond demonstrates better transport characteristics, which is beneficial for fabricating high performance RF MOSFETs.

The off-state breakdown characteristics of the device were measured at V_{GS} of 18 V and a high breakdown voltage of 117 V was obtained, as shown in Fig. 5. It can be observed that the gate leakage current before breakdown was as low as 10^{-7} mA/mm, which is about four orders of magnitude smaller than the off-state drain leakage current. However, when the drain voltage was approaching 117 V, both the

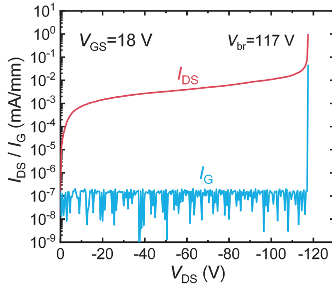

FIGURE 5. The breakdown characteristics of the H-diamond MOSFETs with V_{GS} biased at 18 V.

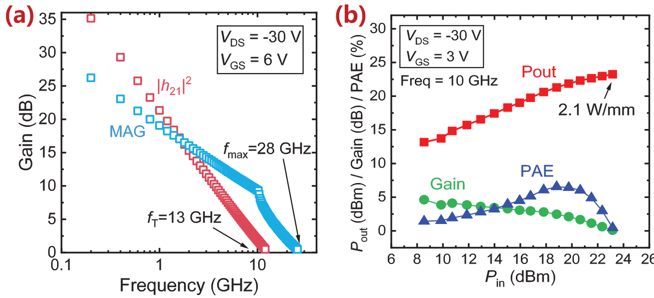

FIGURE 6. (a) The RF small signal characteristics and (b) the RF power output characteristics at 10 GHz of the H-diamond MOSFET with L_G of 0.5 μm.

drain and the gate leakage current demonstrated a sudden increase, indicating the breakdown was mainly occurred on the Al_2O_3 gate dielectric.

The small signal characteristics of the H-diamond MOSFET with gate length of 0.5 μm were measured from 200 MHz to 66 GHz with a step of 200 MHz by a Keysight N5227B vector network analyzer, as the results shown in Fig. 6(a). When the current gain $|h_{21}|^2$ and maximum available gain MAG were decreased to unit, the frequencies were defined as the current gain cutoff frequency f_T and the maximum oscillation frequency f_{max}, respectively. At V_{DS} of -30 V and V_{GS} of 6 V, the extrinsic f_T and f_{max} without de-embedding of 13 GHz and 28 GHz were obtained. Comparing with that on the (001)-oriented diamond in our previous work, both the f_T and f_{max} were improved despite the gate length was increased from 0.35 μm to 0.5 μm. However, as the T-shaped gate was employed, the cutoff frequency f_T was reduced for its significantly increased parasitic capacitance comparing with that with a rectangular shaped gate [20]. The measurement of power output characteristics of the device was carried out at frequency of 10 GHz by an on-wafer load-pull setup and the drain and gate were biased at -30 V and 3 V, respectively. A record high output power density of 2.1 W/mm was achieved at 10 GHz, as shown in Fig. 6(b). The maximum gain and PAE were 4.6 dB and 6.5%, respectively. Comparing with that in our previous work [14], the PAE was reduced, which may be attributed to its high quiescent DC power.

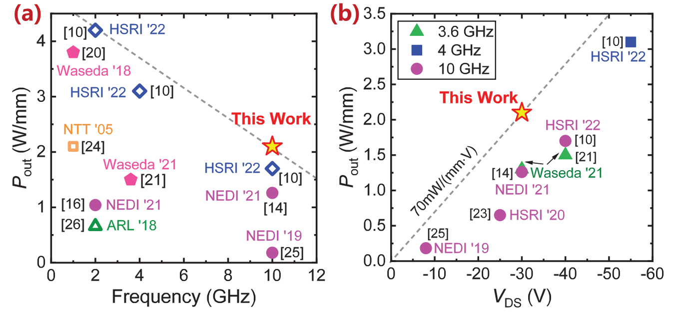

FIGURE 7. (a) The output power density as a function of the operating frequency, and (b) the output power density versus the operating voltage V_{DS} of the H-diamond MOSFETs.

The output power densities of the H-diamond MOSFETs at various operating frequencies are demonstrated in Fig. 7(a) [10], [14], [16], [20], [21], [24], [25], [26]. It can be observed that the output power density was decreased with the increase in operating frequency. At frequency of 10 GHz, we achieved a record high output power density of 2.1 W/mm attributing to the high performance 2DHG channels on (111)-oriented diamond, which is much larger than that of 1.26 W/mm on the (100)-oriented diamond in our previous work. Owing to the low carrier mobility, the H-diamond MOSFET usually demonstrates a high on-resistance and a low current density. Thus, a high operating voltage is usually applied to achieve a high output power density. The power output characteristics of the H-diamond MOSFETs operating at high frequency of 3.6 GHz to 10 GHz are plotted in Fig. 7(b) [10], [14], [21], [23], [25]. It is obvious that the output power density is directly proportional to the operating voltage V_{DS}. For the device operating at 3.6 GHz and 10 GHz, the output power densities of 1.5 W/mm and 1.7 W/mm were obtained at V_{DS} of -40 V, respectively. When the V_{DS} was increased to -55 V, the output power density at 4 GHz was improved to 3.1 W/mm. It indicates that the unit operating voltage contributes to an output power density of 56 mW/mm averagely. In this work, a high output power density of 2.1 W/mm at 10 GHz was obtained at a much lower V_{DS} of -30 V. The average output power density per unit operating voltage was significantly improved to 70 mW/mm. It implies that the performance of 2DHG channels on (111)-oriented diamond outperforms that on other orientations and a high output power density can be achieved at a low operating voltage for its high current density and low on-resistance.

IV. CONCLUSION

High performance H-diamond MOSFETs with Al_2O_3/Si_3N_4 bi-layer passivation and T-shaped gates have been fabricated on a (111)-oriented single crystal diamond substrate. The passivated 2DHG channel showed a high hole sheet density of 1.0×10^{13} cm^{-2} with a corresponding mobility of 104 cm^2/V·s. Owing to the high carrier density, a low ohmic contact resistance R_c of 0.5 Ω·mm was obtained. The RF

MOSFET with gate length of 0.5 μm exhibited a high drain current density of 750 mA/mm, a low on-resistance of 24 Ω·mm, a high maximum oscillation frequency of 28 GHz, as well as a high breakdown voltage of 117 V. Attributing to these excellent properties, a record high output power density of 2.1 W/mm at 10 GHz was realized at a low operating voltage of −30 V, showing a much larger average output power density per unit operating voltage than that on other orientations. These results indicate that the (111)-oriented H-diamond shows great potential for high-frequency and high-power diamond RF MOSFETs.

REFERENCES

[1] C. J. H. Wort and R. S. Balmer, "Diamond as an electronic material," *Mater. Today*, vol. 11, nos. 1–2, pp. 22–28, 2008, doi: 10.1016/S1369-7021(07)70349-8.

[2] N. Donato, N. Rouger, J. Pernot, G. Longobardi, and F. Udrea, "Diamond power devices: State of the art, modelling, figures of merit and future perspective," *J. Phys. D, Appl. Phys.*, vol. 53, no. 9, 2020, Art. no. 93001, doi: 10.1088/1361-6463/ab4eab.

[3] J. Isberg and G. A. Scarsbrook, "High carrier mobility in single-crystal plasma-deposited diamond," *Science*, vol. 297, no. 5587, pp. 1670–1672, 2002, doi: 10.1126/science.1074374.

[4] A. Traoré, S. Koizumi, and J. Pernot, "Effect of n- and p-type doping concentrations and compensation on the electrical properties of semiconducting diamond," *Physica Status Solidi (A)*, vol. 213, no. 8, pp. 2036–2043, 2016, doi: 10.1002/pssa.201600407.

[5] J. Liu, T. Teraji, B. Da, and Y. Koide, "Boron-doped diamond MOSFETs with high output current and extrinsic transconductance," *IEEE Trans. Electron Devices*, vol. 68, no. 8, pp. 3963–3967, Aug. 2021, doi: 10.1109/TED.2021.3087115.

[6] J. Liu, T. Teraji, B. Da, and Y. Koide, "Electrical properties of boron-doped diamond MOSFETs with ozone as oxygen precursor for Al_2O_3 deposition," *IEEE Trans. Electron Devices*, vol. 70, no. 5, pp. 2199–2203, May 2023, doi: 10.1109/ted.2023.3256349.

[7] H. Kawarada, M. Aoki, and M. Ito, "Enhancement mode metal-semiconductor field effect transistors using homoepitaxial diamonds," *Appl. Phys. Lett.*, vol. 65, no. 12, pp. 1563–1565, 1994, doi: 10.1063/1.112915.

[8] X. Yu, J. Zhou, C. Qi, Z. Cao, Y. Kong, and T. Chen, "A high frequency hydrogen-terminated diamond MISFET with f_T/f_{max} of 70/80 GHz," *IEEE Electron Device Lett.*, vol. 39, no. 9, pp. 1373–1376, Sep. 2018, doi: 10.1109/led.2018.2862158.

[9] K. Ueda et al., "Diamond FET using high-quality polycrystalline diamond with f_T of 45 GHz and f_{max} of 120 GHz," *IEEE Electron Device Lett.*, vol. 27, no. 7, pp. 570–572, Jul. 2006, doi: 10.1109/led.2006.876325.

[10] C. Yu et al., "Hydrogen-terminated diamond MOSFETs on (0 0 1) single crystal diamond with state of the art high RF power density," *Funct. Diamond*, vol. 2, no. 1, pp. 64–70, 2022, doi: 10.1080/26941112.2022.2082853.

[11] K. Hirama, H. Takayanagi, S. Yamauchi, J. H. Yang, H. Kawarada, and H. Umezawa, "Spontaneous polarization model for surface orientation dependence of diamond hole accumulation layer and its transistor performance," *Appl. Phys. Lett.*, vol. 92, no. 11, 2008, Art. no. 112107, doi: 10.1063/1.2889947.

[12] K. Hirama et al., "High-performance P-channel diamond metal–oxide–semiconductor field-effect transistors on H-terminated (111) surface," *Appl. Phys. Exp.*, vol. 3, no. 4, 2010, Art. no. 44001, doi: 10.1143/apex.3.044001.

[13] K. Kudara et al., "Over 1 A/mm drain current density and 3.6 W/mm output power density in 2DHG diamond MOSFETs with highly doped regrown source/drain," *Carbon*, vol. 188, pp. 220–228, Mar. 2022, doi: 10.1016/j.carbon.2021.11.034.

[14] X. Yu et al., "1.26 W/mm output power density at 10 GHz for Si_3N_4 passivated H-terminated diamond MOSFETs," *IEEE Trans. Electron Devices*, vol. 68, no. 10, pp. 5068–5072, Oct. 2021, doi: 10.1109/ted.2021.3105622.

[15] X. Yu, J. Zhou, S. Zhang, Z. Cao, Y. Kong, and T. Chen, "H-terminated diamond RF MOSFETs with AlO_x/SiN_x bi-layer passivation and selectively etched T-shaped gates," *Diamond Related Mater.*, vol. 110, Dec. 2020, Art. no. 108160, doi: 10.1016/j.diamond.2020.108160.

[16] X. Yu et al., "1 W/mm output power density for H-terminated diamond MOSFETs with Al_2O_3/SiO_2 bi-layer passivation at 2 GHz," *IEEE J. Electron Devices Soc.*, vol. 9, pp. 160–164, 2021, doi: 10.1109/jeds.2020.3046603.

[17] R. Winter, J. Ahn, P. C. McIntyre, and M. Eizenberg, "New method for determining flat-band voltage in high mobility semiconductors," *J. Vacuum Sci. Technol. B, Nanotechnol. Microelectron. Mater., Process., Meas. Phenomena*, vol. 31, no. 3, 2013, Art. no. 30604, doi: 10.1116/1.4802478.

[18] K. Hirama, H. Takayanagi, S. Yamauchi, J. H. Yang, H. Umezawa, and H. Kawarada, "Channel mobility evaluation for diamond MOSFETs using gate-to-channel capacitance measurement," *Diamond Related Mater.*, vol. 17, nos. 7–10, pp. 1256–1258, 2008, doi: 10.1016/j.diamond.2008.02.031.

[19] M. Kasu, K. Hirama, K. Harada, and T. Oishi, "Study on capacitance–voltage characteristics of diamond field-effect transistors with NO_2 hole doping and Al_2O_3 gate insulator layer," *Jpn. J. Appl. Phys.*, vol. 55, no. 4, 2016, Art. no. 41301, doi: 10.7567/jjap.55.041301.

[20] S. Imanishi et al., "3.8 W/mm power density for ALD Al_2O_3-based two-dimensional hole gas diamond MOSFET operating at saturation velocity," *IEEE Electron Device Lett.*, vol. 40, no. 2, pp. 279–282, Feb. 2019, doi: 10.1109/led.2018.2886596.

[21] K. Kudara et al., "High output power density of 2DHG diamond MOSFETs with thick ALD-Al_2O_3," *IEEE Trans. Electron Devices*, vol. 68, no. 8, pp. 3942–3949, Aug. 2021, doi: 10.1109/TED.2021.3086457.

[22] H. Kawarada, "High-current metal oxide semiconductor field-effect transistors on h-terminated diamond surfaces and their high-frequency operation," *Jpn. J. Appl. Phys.*, vol. 51, no. 9R, 2012, Art. no. 90111, doi: 10.1143/jjap.51.090111.

[23] C. Yu et al., "650 mW/mm output power density of H-terminated polycrystalline diamond MISFET at 10 GHz," *Electron. Lett.*, vol. 56, no. 7, pp. 334–335, 2020, doi: 10.1049/el.2019.4110.

[24] M. Kasu, K. Ueda, H. Ye, Y. Yamauchi, S. Sasaki, and T. Makimoto, "2 W/mm output power density at 1 GHz for diamond FETs," *Electron. Lett.*, vol. 41, no. 22, p. 1249, 2005, doi: 10.1049/el:20053194.

[25] X. Yu, J. Zhou, S. Zhang, Z. Cao, Y. Kong, and T. Chen, "High frequency H-diamond MISFET with output power density of 182mW/mm at 10GHz," *Appl. Phys. Lett.*, vol. 115, no. 19, 2019, Art. no. 192102, doi: 10.1063/1.5125771.

[26] T. G. Ivanov, J. Weil, P. B. Shah, A. G. Birdwell, K. Kingkeo, and E. A. Viveiros, "Diamond RF transistor technology with ft=41 GHz and fmax=44 GHz," in *Proc. IEEE/MTT-S Int. Microw. Symp.*, 2018, pp. 1461–1463, doi: 10.1109/MWSYM.2018.8439521.